IMA Journal of Applied Mathematics (2013) Page 1 of 15
doi:10.1093/imamat/hxt030

A mathematical model for the keratin cycle of assembly and disassembly

Chengjun Sun
Department of Mathematics, University of Manitoba, Winnipeg, MB, Canada R3T 2N2

Rudolf Leube
Institute of Molecular and Cellular Anatomy, RWTH Aachen University, 52074 Aachen, Germany

Reinhard Windoffer
Institute of Molecular and Cellular Anatomy, RWTH Aachen University, 52074 Aachen, Germany

and

Stéphanie Portet*
Department of Mathematics, University of Manitoba, Winnipeg, MB, Canada R3T 2N2
*Corresponding author: portets@cc.umanitoba.ca

[Received on 17 May 2012; revised on 29 April 2013; accepted on 29 April 2013]

We formulate a mathematical model to study the *in vivo* keratin organization in terms of repartition of the keratin material between three different structural states: soluble proteins, filament precursors and filamentous state. The model describes a cycle of assembly and disassembly of keratin material. A generic nucleation function and structural stability of filament precursors are assumed. It is established that the three structural states always coexist and that the repartition of keratin material never exhibits any cyclic behaviour. Under some conditions, it is shown that the choice of the nucleation function does not affect the qualitative behaviour of the system. However, it might change the stable repartition of the keratin material in the cell.

Keywords: intermediate filaments; cytoskeleton assembly dynamics; index theory; globally asymptotically stable.

1. Introduction

The cytoskeleton in epithelial cells is composed of three major filament systems: actin-based microfilaments, tubulin-based microtubules and keratin-based intermediate filaments. Keratin intermediate filaments differ from the other filament types by their lack of polarity, their high degree of phosphorylation, compositional diversity, extreme elasticity and their propensity to spontaneously assemble *in vitro* without any co-factors (reviews in Herrmann *et al.*, 2007; Kim & Coulombe, 2007; Magin *et al.*, 2007). Very little is known about the regulation of the *in vivo* keratin assembly needed to establish, maintain and functionally adapt the complex and evolutionary conserved network arrangements observed in different epithelial cell types (e.g. Carberry *et al.*, 2009; Iwatsuki & Suda, 2010; Oriolo *et al.*, 2007). Live cell imaging has revealed a surprisingly high degree of network plasticity, most notably in the context of various stress paradigms (Beriault *et al.*, 2012; Sivaramakrishnan *et al.*, 2009; Strnad *et al.*, 2001, 2002; Windoffer *et al.*, 2004; Woll *et al.*, 2007). Based on such observations in various cell culture systems, a model has been put forward to explain the time-dependent regulation of keratin networks (Leube *et al.*, 2011; Windoffer *et al.*, 2011). Its main tenet is that keratin filaments are subject to continuous

assembly and disassembly and that this cycling, which is independent of protein biosynthesis, is subject to modulation depending on the specific context-dependent requirements.

The keratin cycle of assembly and disassembly consists of distinct steps that occur in defined topologies and sequential order (for details and references see Kolsch *et al.*, 2010; Leube *et al.*, 2011; Windoffer *et al.*, 2011). Thus, nucleation of keratin particles, which are referred to as keratin filament precursors, preferentially takes place in the cell periphery and appears to be linked to focal adhesions. These adhesion sites are implicated in attachment of cells to the extracellular matrix and are needed for cell migration. It is assumed that keratin tetramers and/or higher order oligomers that have been identified in the soluble cytoplasmic pool assemble into small filamentous particles in close proximity to focal adhesions. These keratin filament precursor particles grow by addition of oligomers to either end. At the same time, they are transported from the cell periphery towards the cell interior. This transport is primarily supported by actin filaments. Once particles approach the peripheral keratin network, they integrate by end-on insertion. Keratin filaments within the network further translocate towards the nucleus with the help of actin filaments and microtubules. They bundle and either form a stable cage-like network around the nucleus or disassemble giving rise to soluble subunits that can be re-utilized for another round of assembly and disassembly.

The goal of the current modelling attempt is to describe, in mathematical terms, aspects of the keratin cycle that can be used to correlate experimental measurements with the hypotheses put forward to analyse keratin network plasticity in quantitative terms. This endeavour will help us to understand and define the various stress responses of the keratin system and the kinetic differences of keratin isotypes in different cellular environments.

In a previous work, Portet & Arino (2009) developed an *in vivo* intermediate filament model and investigated the dynamic properties of intermediate filament material organization in terms of repartition between four different structural states: soluble proteins, particles, and short and long filaments. By means of sensitivity analysis, post-translational modifications of intermediate filament proteins resulting in filament solubilization are found, in agreement with biological observations, to be the main regulator of the intermediate filament organization in cells (Woll *et al.*, 2007).

In the current model, it is assumed as in Portet & Arino (2009) that the cell is spatially homogeneous; events are not spatially localized and transport of the keratin material within the cell is not described. However, the present model is a refinement of the model in Portet & Arino (2009) that accounts for the recent biological observations (Kolsch *et al.*, 2010; Leube *et al.*, 2011; Windoffer *et al.*, 2011). In the previous work, a distinction was made between short and long filaments. It has been shown since that filaments of any length behave similarly, assembling by end to end aggregation (Colakoglu & Brown, 2009; Winheim *et al.*, 2011); hence, all filaments are considered here as elements of the same structural state, the filamentous state. Therefore, the current model categorizes materials as follows: soluble proteins, filament precursors (previously called particles) and filamentous state. Moreover, in Portet & Arino (2009), a specific expression for the nucleation of particles (or filament precursors) was used, assuming that the collision of n soluble proteins (tetramers) results in the formation of a particle. Values of n up to 8 were considered to represent the well-documented formation of unit-length filaments (ULFs) by lateral aggregation of eight tetramers observed in the *in vitro* assembly of intermediate filaments of vimentin type (Herrmann & Aebi, 2004). It is assumed here that the nucleation function is a generic function, hypothesizing only a non-decreasing dependence on soluble protein concentration. This relaxation of assumptions on the nucleation process was made as the *in vivo* nucleation mechanisms are still poorly understood and could be more sophisticated than the *in vitro* nucleation mechanisms that were assumed in Portet & Arino (2009). Moreover, filament precursors are assumed here to be structurally stable; no disassembly of filament precursors is posited. Finally, based on observations made by

experimentalists, the formation of elements of the filamentous state is now described by the aggregation or fusion of filament precursors as well as precursors to filaments (Kolsch *et al.*, 2010; Leube *et al.*, 2011; Windoffer *et al.*, 2011).

Hence, a 3D system of ordinary differential equations is proposed to describe the organization of the keratin material in a cell. The keratin assembly/disassembly cycle in cells is assumed to consist of mechanisms of precursor formation and growth, integration of precursors in the filamentous state and disassembly of the filamentous state into soluble proteins. The bundling process is not explicitly represented in the model as it does not change the repartition of keratin material in cells. Analytical analysis of the system is presented. Results are found on the bounds of filamentous and non-filamentous states and long-term behaviour of the repartition of the keratin material in the cells.

2. Model formulation

To describe the organization of keratin in a cell, the keratin material is categorized in three structural states: soluble proteins (tetrameric complexes), filament precursors (oligomeric particles of soluble proteins) and filamentous state (filaments forming the network). The three state variables to represent structural states are

- $S(t)$, *soluble protein* concentration at time t;
- $P(t)$, *filament precursor* concentration at time t;
- $N(t)$, *filamentous state* concentration at time t.

In the present model, the configuration and size of objects considered are not explicitly described. Only interactions (events) linking the three structural states are used to define their properties. The following five events are assumed to govern the dynamics of keratin material in an epithelial cell (Fig. 1):

- Formation of filament precursors, called here *Nucleation*: soluble proteins oligomerize to form filament precursors.
- *Growth* of precursors: soluble proteins bind to filament precursors.
- *Integration I*: fusion/aggregation of precursors forms an element of the filamentous state.

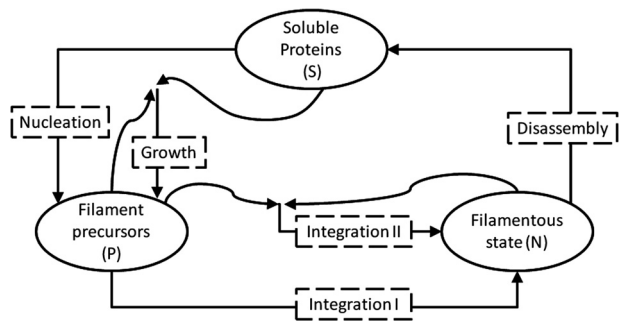

FIG. 1. Interactions between structural states governing the cycle of keratin material in a cell. Soluble proteins (tetramers) oligomerize and form filament precursors (Nucleation). Filament precursors grow by the binding of soluble proteins (Growth). Filament precursors fuse and form filaments (Integration I). Filament precursors can also integrate to the filamentous state (Integration II). Finally, filaments (filamentous state) disassemble into soluble proteins (Disassembly).

TABLE 1 *Parameters and function used in system* (2.1)

Parameters	Signification
$\mathcal{N}(S)$	Nucleation function
π	Rate of growth of filament precursors
κ	Rate of disassembly of filamentous state
β	Rate of fusion of precursors (Integration I)
i	Rate of integration of precursors to filamentous state (Integration II)

- *Integration II*: precursors aggregate to existing filaments or network (filamentous state).
- *Disassembly*: elements of the filamentous state disassemble into soluble proteins.

Based on assumptions listed above, the model describing the dynamics of the keratin material in a cell is

$$\frac{\mathrm{d}S}{\mathrm{d}t} = -\mathcal{N}(S) - \pi SP + \kappa N, \tag{2.1a}$$

$$\frac{\mathrm{d}P}{\mathrm{d}t} = \mathcal{N}(S) + \pi SP - iPN - \beta P^2, \tag{2.1b}$$

$$\frac{\mathrm{d}N}{\mathrm{d}t} = iPN + \beta P^2 - \kappa N. \tag{2.1c}$$

Parameters in system (2.1) are all positive: i, β and π are the integration rate, the fusion rate and the growth rate of filament precursors, respectively; κ is the disassembly rate of filamentous state (Table 1). Moreover, as little is known on the *in vivo* oligomerization of intermediate filament proteins, called here nucleation, a generic function $\mathcal{N}(\cdot)$ is used to describe the nucleation process. It is assumed that the nucleation function $\mathcal{N}(S)$ is continuously differentiable, and satisfies:

– $\mathcal{N}'(S) \geqslant 0$ for $S \in [0, C_0]$, where C_0 is the concentration of keratin in a cell. The nucleation function is a monotonically increasing function of the concentration of soluble proteins. Saturating and non-saturating functions can be hypothesized.

– $\mathcal{N}(0) = 0$ (no nucleation possible if no soluble proteins).

Parameters and function used in system (2.1) are listed in Table 1. System (2.1) is considered with initial conditions $S(0)$, $P(0)$, $N(0) \geqslant 0$ and $S(0) + P(0) + N(0) = C_0$. System (2.1) satisfies a mass conservation law, $S(t) + P(t) + N(t) = C_0 \ \forall t \geqslant 0$.

3. Mathematical analysis

To allow for an easier interpretation of results of the keratin material repartition in cells, the non-dimensional version of system (2.1) is considered and obtained by making the transformations $\bar{S} = S/C_0$, $\bar{P} = P/C_0$, $\bar{N} = N/C_0$. The new state variables $\bar{S}$, $\bar{P}$ and $\bar{N}$ are the proportions of keratin material in the form of soluble proteins, filament precursors and filamentous state in the cell. System (2.1) is now

replaced by

$$\frac{\mathrm{d}S}{\mathrm{d}t} = -\frac{\mathcal{N}(C_0 S)}{C_0} - \pi C_0 SP + \kappa N, \tag{3.1a}$$

$$\frac{\mathrm{d}P}{\mathrm{d}t} = \frac{\mathcal{N}(C_0 S)}{C_0} + \pi C_0 SP - iC_0 PN - \beta C_0 P^2, \tag{3.1b}$$

$$\frac{\mathrm{d}N}{\mathrm{d}t} = iC_0 PN + \beta C_0 P^2 - \kappa N, \tag{3.1c}$$

after omitting the bars over the new variables $\bar{S}, \bar{P}, \bar{N}$. System (3.1) is well-posed. It can be verified that the set $\mathscr{D}_1 := \{(S,P,N) \in \mathbb{R}^3_+ \mid S+P+N=1\}$ is positively invariant with respect to system (3.1). Solutions are uniformly bounded on $\mathscr{D}_1$.

The conservation law $S+P+N=1$ allows one to attack system (3.1) by studying the subsystem

$$\frac{\mathrm{d}S}{\mathrm{d}t} = -\frac{\mathcal{N}(C_0 S)}{C_0} - \pi C_0 SP + \kappa(1-S-P) =: f_1(S,P), \tag{3.2a}$$

$$\frac{\mathrm{d}P}{\mathrm{d}t} = \frac{\mathcal{N}(C_0 S)}{C_0} + \pi C_0 SP - iC_0 P(1-S-P) - \beta C_0 P^2 =: f_2(S,P), \tag{3.2b}$$

and determine N from $N = 1-S-P$. Define $\mathscr{D}_2 := \{(S,P) \in \mathbb{R}^2_+ \mid 0 \leqslant S+P \leqslant 1\}$. One can verify that $\mathscr{D}_2$ is positively invariant with respect to system (3.2).

The next result gives finer bounds for the long-term behaviour of the non-filamentous and filamentous states.

LEMMA 3.1 For all sufficiently large t, the non-filamentous state $S(t)+P(t)$ and the filamentous state $N(t)$ satisfy

$$\max\left(0, 1 - \frac{C_0(i+\beta)}{\kappa}\right) \leqslant S(t)+P(t) \leqslant 1$$

and

$$0 \leqslant N(t) \leqslant \min\left(1, \frac{C_0(i+\beta)}{\kappa}\right).$$

Proof. Denote $Z := S+P$. Adding up (3.2a) and (3.2b) yields

$$\mathrm{d}Z/\mathrm{d}t = \kappa - iC_0 P - \beta C_0 P^2 - (\kappa - iC_0 P)Z,$$

which, as $0 \leqslant P(t) \leqslant 1 \ \forall t \geqslant 0$, implies that

$$\kappa - C_0(i+\beta) - \kappa Z \leqslant \frac{\mathrm{d}Z}{\mathrm{d}t}.$$

Integrating each side of the inequality gives

$$1 - \frac{C_0(i+\beta)}{\kappa} + \left(Z(0) - 1 + \frac{C_0(i+\beta)}{\kappa}\right)\mathrm{e}^{-\kappa t} \leqslant Z(t).$$

As $0 \leqslant Z(t) \leqslant 1\ \forall t \geqslant 0$, $Z(t)$ satisfies

$$\max\left(0, 1 - \frac{C_0(i+\beta)}{\kappa} + \left(Z(0) - 1 + \frac{C_0(i+\beta)}{\kappa}\right)\mathrm{e}^{-\kappa t}\right) \leqslant Z(t) \leqslant 1 \quad \forall t \geqslant 0.$$

Now considering t sufficiently large, the first inequality in the result follows. Since $N(t) = 1 - Z(t)$,

$$0 \leqslant N(t) \leqslant 1 - \max\left(0, 1 - \frac{C_0(i+\beta)}{\kappa}\right)$$

for all sufficiently large t. Therefore,

$$0 \leqslant N(t) \leqslant \min\left(1, \frac{C_0(i+\beta)}{\kappa}\right)$$

for all sufficiently large t. □

Interpretation: Balance between the fusion of precursors (Integration I), integration of precursors to filamentous state (Integration II) and disassembly of filamentous state (see Fig. 1) plays a key role in the long-term repartition of keratin material between the non-filamentous states (S and P) and the filamentous state (N). The ratio of rates of filamentous state assembly (i and β) to the rate of filamentous state disassembly (κ) determines the organization of the material between filamentous and non-filamentous states in the long run. Note that the higher the disassembly rate κ, the lower the proportion of the keratin material assembled in the filamentous state. *In vivo* disassembly of the filamentous pool is due to post-transcriptional modifications of proteins triggered, for instance, by kinase activity; see, e.g. Woll *et al.* (2007).

As a generic function $\mathcal{N}(\cdot)$ is used to describe the nucleation process, a complete characterization of equilibria of system (3.2) is difficult. The next three results (Theorems 3.1–3.3) give some information on the equilibrium existence and values.

THEOREM 3.1 System (3.2) does not possess the trivial equilibrium $(0, 0)$, or any boundary equilibria $(S, 0)$ and $(0, P)$.

Theorem 3.1 can be verified by setting the right-hand side of system (3.2) to zero. Here, we omit the details.

THEOREM 3.2 System (3.2) has at least one interior equilibrium, denoted by (S_*, P_*), in $\mathscr{D}_2$.

Proof. Regard the boundary of $\mathscr{D}_2$ (formed by the vertical line $S = 0$, the horizontal line $P = 0$ and the line $S + P = 1$), denoted by Γ, as a Jordan curve. Denote by $I_{(f_1,f_2)^\top}(\Gamma)$ the index of Γ relative to the vector field, defined in system (3.2), $(f_1, f_2)^\top \in C^1(\mathbb{R}^2)$. Since $\mathscr{D}_2$ is a 2D positively invariant set with respect to system (3.2), it follows that $I_{(f_1,f_2)^\top}(\Gamma) = 1$. One can also refer to the vector field of (3.2) at each point of the closed loop Γ in Fig. 2. By Index Theory (Perko, 2001, Theorem 1, p. 301), there exists at least one equilibrium inside $\mathscr{D}_2$. □

THEOREM 3.3 Interior equilibria (S_*, P_*) of system (3.2) can be characterized as follows:

- if $i = \beta$, $(S_*, P_*) = (1 - \kappa P_*/(\kappa - iC_0P_*), P_*)$, with $P_* \in (0, \kappa/(\kappa + iC_0))$;
- if $i \neq \beta$, $(S_*, P_*) = (1 + P_*(C_0(i-\beta)P_* - \kappa)/(\kappa - iC_0P_*), P^*)$,

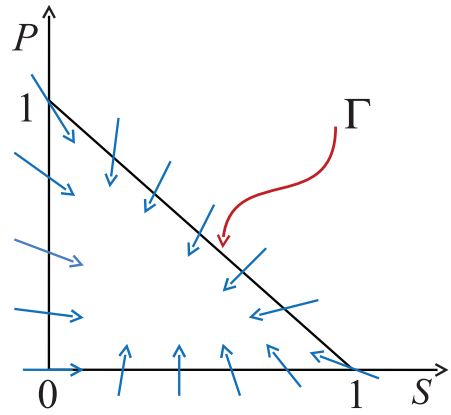

FIG. 2. Vector field of system (3.2) on the Jordan curve Γ.

– with $P_* \in (0, \min(\kappa/iC_0, \left(-(\kappa + iC_0) - \sqrt{(\kappa - iC_0)^2 + 4\kappa C_0\beta}\right)/2C_0(i-\beta), 1))$, if $i < \beta$,

– with $P_* \in (0, \min(\kappa/(i-\beta)C_0, 1))$, if $i > \beta$.

Proof. Equilibrium (S_*, P_*) of system (3.2) satisfies $f_1(S_*, P_*) = 0$ and $f_2(S_*, P_*) = 0$. Adding $f_1(S_*, P_*) = 0$ and $f_2(S_*, P_*) = 0$ leads to

$$\kappa(1 - S_* - P_*) - iC_0P_*(1 - S_* - P_*) - \beta C_0P_*^2 = 0. \tag{3.3}$$

Fixing P_* in (3.3), and solving (3.3) for S_* gives a linear equation in S_* whose the solution is

$$S_* = 1 + \frac{P_*\,(C_0(i-\beta)P_* - \kappa)}{\kappa - iC_0P_*}. \tag{3.4}$$

From Theorem 3.2, there is at least one interior equilibrium inside $\mathcal{D}_2$. To satisfy $0 < S_* < 1$, (3.4) leads to the following conditions

- with $i = \beta$

$$\frac{\kappa P_*}{\kappa - iC_0P_*} < 1 < 1 + \frac{\kappa P_*}{\kappa - iC_0P_*}.$$

  The right-hand side of the inequality is satisfied for $P_* < \kappa/iC_0$; then the left-hand side is satisfied for $P_* < \kappa/(\kappa + iC_0) < \kappa/iC_0$.

- with $i \neq \beta$

$$-\frac{\kappa P_*(C_0(i-\beta)P_* - \kappa)}{\kappa - iC_0P_*} < 1 < 1 - \frac{\kappa P_*(C_0(i-\beta)P_* - \kappa)}{\kappa - iC_0P_*}. \tag{3.5}$$

  The right-hand side of the inequality (3.5) is satisfied when $\kappa P_*(C_0(i-\beta)P_* - \kappa)/(\kappa - iC_0P_*) < 0$. The left-hand side of the inequality (3.5) depends on the sign of the quadratic function

$Q(P_*) = -C_0(i-\beta)P_*^2 + (\kappa + iC_0)P_* - \kappa$, having two real roots

$$P_{*_{1,2}} = \frac{-(\kappa + iC_0) \pm \sqrt{(\kappa + iC_0)^2 - 4\kappa(i-\beta)C_0}}{2C_0(i-\beta)} = \frac{-(\kappa + iC_0) \pm \sqrt{(\kappa - iC_0)^2 + 4\kappa\beta C_0}}{2C_0(i-\beta)}.$$

- For $i < \beta$: The right-hand side of the inequality (3.5) is satisfied for $P_* < \kappa/iC_0$. Satisfying the left-hand side of (3.5) is equivalent to satisfying $Q(P_*) < 0$. By Descartes' rule of signs, it is found that $Q(P_*)$ has exactly one negative and one positive real root, respectively, P_{*_1} and P_{*_2}. As the leading coefficient of $Q(P_*)$ is positive, its graph is a concave-up parabola, hence the left-hand side of (3.5) is satisfied for $P_* \in (0, P_{*_2} = (-(\kappa + iC_0) - \sqrt{(\kappa - iC_0)^2 + 4\kappa C_0\beta})/2C_0(i-\beta))$.
- For $i > \beta$: Two cases have to be considered:
  - The right-hand side of the inequality (3.5) is satisfied when $\kappa - iC_0P_* < 0$ and $C_0(i-\beta)P^* - \kappa > 0$; these two conditions lead to $P_* > \kappa/C_0(i-\beta)$. With $\kappa - iC_0P_* < 0$, the left-hand side of (3.5) is equivalent to $Q(P_*) > 0$. Both roots $P_{*_{1,2}}$ are negative and the leading coefficient of $Q(P_*)$ is negative. Hence, the left-hand side of (3.5) cannot be satisfied for any positive value of P_*. This case is not possible.
  - The right-hand side of the inequality (3.5) is satisfied when $\kappa - iC_0P_* > 0$ and $C_0(i-\beta)P^* - \kappa < 0$; these two conditions lead to $P_* < \kappa/C_0(i-\beta)$. With $\kappa - iC_0P_* > 0$, the left-hand side of (3.5) is equivalent to satisfy $Q(P_*) < 0$. Both roots $P_{*_{1,2}}$ are negative and the leading coefficient of $Q(P_*)$ is negative. Hence, the left-hand side of (3.5) is satisfied for any positive value of P_*. Hence, the inequality (3.5) is satisfied for $P_* < \kappa/C_0(i-\beta)$. □

Note that the equilibrium values are mainly determined by κ, i and β, as are the bounds of solutions in long run (Lemma 3.1).

The next result excludes the existence of periodic solutions.

THEOREM 3.4 System (3.2) has no periodic solutions, homoclinic loops or oriented phase polygons inside the region $\mathscr{D}_2$.

Proof. To prove this theorem, we apply the approach developed by Li (1996). For system (3.1) on the positively invariant pyramid $\mathscr{D}_1$, one can show from Theorem 3.1 that there are no boundary equilibria; the vector field traverses strictly inwards along the boundary of $\mathscr{D}_1$ due to its property of positive invariance; solutions to system (3.1) are uniformly bounded on $\mathscr{D}_1$; $\mathscr{D}_1$ is simply connected. These characteristics imply that system (3.1) is uniformly persistent in $\mathscr{D}_1$, and thus there is a compact absorbing set $K \subset \mathscr{D}_1$.

Define the vector field of system (3.1) as $\mathbf{f}$. Calculating the divergence of system (3.1) gives

$$\nabla \cdot \mathbf{f} = -\mathcal{N}'(C_0S) - \pi C_0P + \pi C_0S - iC_0N - 2\beta C_0P + iC_0P - \kappa,$$

where the prime ($'$) stands for the derivative with respect to C_0S. Transforming equations (3.1b) and (3.1c) yields

$$\pi C_0 S - iC_0 N - \beta C_0 P = \frac{P'}{P} - \frac{\mathcal{N}(C_0 S)}{C_0 P},$$
$$iC_0 P - \kappa = \frac{N'}{N} - \frac{\beta C_0 P^2}{N}.$$

Consequently, the divergence of system (3.1) reduces to

$$\nabla \cdot \mathbf{f} = -\mathcal{N}'(C_0 S) - \pi C_0 P - \beta C_0 P - \frac{\mathcal{N}(C_0 S)}{C_0 P} - \frac{\beta C_0 P^2}{N} + \frac{P'}{P} + \frac{N'}{N}.$$

Take similar notation as in Li (1996): $n, r, \nu, P(\mathbf{x})$ and $I_{M\times M}$, where $\mathbf{x} := (S, P, N)$, $M = \binom{n}{r+2}$ and $P(\mathbf{x})$ is a non-singular $\binom{n}{r+2} \times \binom{n}{r+2}$ matrix-valued function. For $n = 3, r = 1, \nu = 0$, then $M = 1$. Thus $I_{1\times 1} = 1$, $P(\mathbf{x})$ is scalar-valued and

$$P_{\mathbf{f}} P^{-1} + P \frac{\partial \mathbf{f}}{\partial \mathbf{x}}^{[r+2]} P^{-1} - r\nu I_{M\times M} = P_{\mathbf{f}} P^{-1} + P \frac{\partial \mathbf{f}}{\partial \mathbf{x}}^{[3]} P^{-1}$$
$$= \nabla \cdot \mathbf{f},$$

where $P_{\mathbf{f}}$ is obtained by replacing each entry of P by its derivative in the direction of $\mathbf{f}$, and $\partial \mathbf{f}^{[r+2]}/\partial \mathbf{x}$ is the $(r+2)$th additive compound matrix of the Jacobian matrix $\partial \mathbf{f}/\partial \mathbf{x}$. Thus, the quantity $\bar{q}_{r+2}$ used in the condition in Li (1996, Theorem 2.3), depends only on the divergence of system (3.1).

Let $(S(t), P(t), N(t))$ be any solution starting in the compact absorbing set $K \subset \mathscr{D}_1$. Along $(S(t), P(t), N(t))$, we have

$$\begin{aligned}
\frac{1}{t}\int_0^t \nabla \cdot \mathbf{f}\, \mathrm{d}t &= -\frac{1}{t}\int_0^t \left[\mathcal{N}'(C_0 S) + \pi C_0 P + \beta C_0 P + \frac{\mathcal{N}(C_0 S)}{C_0 P} + \frac{\beta C_0 P^2}{N}\right] \mathrm{d}t \\
&\quad + \frac{1}{t}\int_0^t \left[\frac{P'}{P} + \frac{N'}{N}\right] \mathrm{d}t \\
&= -\frac{1}{t}\int_0^t \left[\mathcal{N}'(C_0 S) + \pi C_0 P + \beta C_0 P + \frac{\mathcal{N}(C_0 S)}{C_0 P} + \frac{\beta C_0 P^2}{N}\right] \mathrm{d}t \\
&\quad + \frac{1}{t}\left[\ln \frac{P(t)}{P(0)} + \ln \frac{N(t)}{N(0)}\right] \\
&\leqslant -c < 0
\end{aligned}$$

for all sufficiently large t, where the positive c may depend on the uniformly persistent constant but is independent of initial conditions. The conditions in Li (1996, Theorem 2.3) are then satisfied. The proof is complete. □

In vitro studies have shown that filament precursors, ULFs in the *in vitro* case, behave for the aggregation processes as filaments; ULF is considered as the shortest filament. The ULF end-to-end rate (similar to the fusion rate of precursors) is slightly faster than the rate of aggregation of a ULF to a filament (Portet *et al.*, 2009). Moreover, the previous results seem to indicate that relative values of i

and β might influence the behaviour of system (3.2). Consequently, different cases for β and i are now considered.

3.1 *Case* $\beta = i$

First, the rate of precursor fusion and the rate of integration of precursors to the filamentous state are assumed to be equal and it is postulated that precursors and elements of the filamentous state behave similarly for the assembly process.

THEOREM 3.5 Suppose $\beta = i$. Interior equilibria (S_*, P_*) of system (3.2), where $S_* \in (0, i/(i+\pi))$, are locally asymptotically stable.

Proof. The coordinates of an interior equilibrium (S_*, P_*) satisfy

$$-\frac{\mathcal{N}(C_0 S_*)}{C_0} - \pi C_0 S_* P_* + \kappa(1 - S_* - P_*) = 0, \tag{3.6a}$$

$$\frac{\mathcal{N}(C_0 S_*)}{C_0} + \pi C_0 S_* P_* - iC_0 P_*(1 - S_* - P_*) - \beta C_0 P_*^2 = 0. \tag{3.6b}$$

Solving (3.6a) for P_* in terms of S_* gives

$$P_* = \frac{\kappa(1 - S_*) - \mathcal{N}/(C_0 S_*) C_0}{\kappa + \pi C_0 S_*}. \tag{3.7}$$

Substituting (3.7) into (3.6b), S_* satisfies

$$\begin{aligned}
&\left[1 - \frac{C_0(\pi + i)S_*}{\kappa + \pi C_0 S_*} + \frac{iC_0}{\kappa + \pi C_0 S_*} - \frac{2C_0\kappa(i - \beta)(1 - S_*)}{(\kappa + \pi C_0 S_*)^2}\right] \frac{\mathcal{N}(C_0 S_*)}{C_0} \\
&\quad + \frac{C_0(i - \beta)}{(\kappa + \pi C_0 S_*)^2}\left[\frac{\mathcal{N}(C_0 S_*)}{C_0}\right]^2 + \frac{C_0\kappa(\pi + i)S_*(1 - S_*)}{\kappa + \pi C_0 S_*} - iC_0\frac{\kappa(1 - S_*)}{\kappa + \pi C_0 S_*} \\
&\quad + C_0(i - \beta)\left(\frac{\kappa(1 - S_*)}{\kappa + \pi C_0 S_*}\right)^2 = 0.
\end{aligned} \tag{3.8}$$

When $\beta = i$, equation (3.8) then simplifies to

$$[\kappa + C_0 i(1 - S_*)]\frac{\mathcal{N}(C_0 S_*)}{C_0} + C_0\kappa(1 - S_*)[(i + \pi)S_* - i] = 0. \tag{3.9}$$

One can verify that $S_* \in (0, i/(i+\pi))$.

The Jacobian matrix of system (3.2) at an arbitrary point (S, P) is

$$\mathcal{J}(S, P) = \begin{pmatrix} -\mathcal{N}'(C_0 S) - \pi C_0 P - \kappa & -\pi C_0 S - \kappa \\ \mathcal{N}'(C_0 S) + \pi C_0 P + iC_0 P & \pi C_0 S - iC_0(1 - S - P) + iC_0 P - 2\beta C_0 P \end{pmatrix}.$$

The trace of $\mathcal{J}(S, P)$ is

$$\begin{aligned}
\operatorname{tr}(\mathcal{J}(S, P)) &= -\mathcal{N}'(C_0 S) - \pi C_0 P - \kappa + \pi C_0 S - iC_0(1 - S - P) + iC_0 P - 2\beta C_0 P \\
&= -\mathcal{N}'(C_0 S) - \kappa - iC_0 + C_0(i + \pi)S + C_0(2i - 2\beta - \pi)P.
\end{aligned} \tag{3.10}$$

From (3.10), when $\beta = i$, the trace of $\mathcal{J}(S,P)$ at an interior equilibrium (S_*, P_*) simplifies to

$$\begin{aligned}\operatorname{tr}(\mathcal{J}(S_*,P_*)) &= -\mathcal{N}'(C_0S_*) - \kappa - iC_0 + C_0(i+\pi)S_* - \pi C_0P_* \\ &< -\mathcal{N}'(C_0S_*) - \kappa - iC_0 + C_0(i+\pi)\frac{i}{i+\pi} - \pi C_0P_* \\ &= -\mathcal{N}'(C_0S_*) - \kappa - \pi C_0P_*.\end{aligned}$$

Obviously, $\operatorname{tr}(\mathcal{J}(S_*,P_*)) < 0$ whenever $\mathcal{N}'(C_0S_*) \geqslant 0$.

The determinant of the Jacobian matrix $\mathcal{J}(S,P)$ at an interior equilibrium (S_*, P_*) is

$$\begin{aligned}\det(\mathcal{J}(S_*,P_*)) = {}& \mathcal{N}'(C_0S_*)[\kappa + iC_0(1-S_*)] + C_0(\pi C_0 i + \kappa\pi + \kappa i)P_* \\ & + \kappa C_0[i - (i+\pi)S_*] - 2C_0(i-\beta)P_*(\mathcal{N}'(C_0S_*) + \pi C_0P_* + \kappa).\end{aligned} \tag{3.11}$$

When $\beta = i$, equation (3.11) simplifies to

$$\begin{aligned}\det(\mathcal{J}(S_*,P_*)) &= \mathcal{N}'(C_0S_*)[\kappa + iC_0(1-S_*)] + C_0(\pi C_0 i + \kappa\pi + \kappa i)P_* \\ &\quad + \kappa C_0[i - (i+\pi)S_*] \\ &> \mathcal{N}'(C_0S_*)[\kappa + iC_0(1-S_*)] + \pi C_0^2 iP_* + \kappa\pi C_0P_* + \kappa iC_0P_* \\ &\quad + \kappa C_0\left[i - (i+\pi)\frac{i}{i+\pi}\right] \\ &= \mathcal{N}'(C_0S_*)[\kappa + iC_0(1-S_*)] + \pi C_0^2 iP_* + \kappa\pi C_0P_* + \kappa iC_0P_*.\end{aligned}$$

Based on the assumptions on the nucleation function $\mathcal{N}(S)$, $\mathcal{N}'(C_0S_*) \geqslant 0$ is always true, implying that $\det(\mathcal{J}(S_*,P_*)) > 0$. As $\operatorname{tr}(\mathcal{J}(S_*,P_*)) < 0$ and $\det(\mathcal{J}(S_*,P_*)) > 0$, the result follows. □

Does system (3.2) have multiple interior equilibria under the hypothesis $\beta = i$? The following result gives the answer.

THEOREM 3.6 Suppose $\beta = i$. System (3.2) possesses a unique interior equilibrium (S_*, P_*) in $\mathscr{D}_2$.

Proof. Define the same Jordan curve Γ as in the proof of Theorem 3.2. Then $I_{(f_1,f_2)^\top}(\Gamma)$, the index of Γ relative to the vector field defined in system (3.2) $(f_1,f_2)^\top \in C^1(\mathbb{R}^2)$, is equal to 1. Suppose system (3.2) has interior equilibria $E_1, \cdots, E_q$ $(q \geqslant 2)$. By Index Theory (Perko, 2001, Theorem 2, p. 302), $I_{(f_1,f_2)^\top}(\Gamma) = \sum_{j=1}^{q} I_{(f_1,f_2)^\top}(E_j) = q$ after considering the local asymptotic stability (Theorem 3.5) of these q interior equilibria. However, this contradicts the fact $I_{(f_1,f_2)^\top}(\Gamma) = 1$, implying that system (3.2) has a unique interior equilibrium when $\beta = i$. □

Theorems 3.4–3.6 along with the generalized Poincaré–Bendixson Theorem (Perko, 2001, Theorem 2, p. 245) give the following result.

THEOREM 3.7 Suppose $\beta = i$. The unique interior equilibrium (S_*, P_*) of system (3.2) is globally asymptotically stable in $\mathscr{D}_2$.

REMARK We also can prove Theorem 3.7 by Li (1996, Corollary 3.5) when the interior equilibrium (S_*, P_*) of system (3.2) is unique.

Interpretation of results when $\beta = i$: When precursor fusion and integration of filament precursors to the filamentous state are assumed to be subject to same rates, then regardless of any initial configuration of keratin material, the system always reaches, when time becomes large, a steady repartition in which all keratin structural states coexist (Theorem 3.7). Note that the equilibrium proportion of the soluble proteins S_* is limited by $i/(i+\pi)$ (Theorem 3.5), whereas the equilibrium proportion of filament precursors P_* is limited by $\kappa/(\kappa + iC_0)$ (Theorem 3.3).

3.2 *Case $\beta \neq i$*

When $\beta \neq i$, it is difficult to obtain the number and the stability properties of interior equilibria for system (3.2) due to the general form of nucleation function $\mathcal{N}(C_0 S)$.

THEOREM 3.8 Suppose $\beta > i$. The interior equilibrium (S_*, P_*) is unique and globally asymptotically stable if each interior equilibrium is locally asymptotically stable.

Theorem 3.8 can be proved by the Bendixson criterion (Bendixson, 1901) and the Index Theory (Perko, 2001, Theorem 2, p. 302), similar to the proofs of Theorems 3.6 and 3.7. Here, we omit the details.

THEOREM 3.9 Suppose $\beta > i$. System (3.2) possesses at least three interior equilibria (S_*, P_*) if one of these equilibria is an unstable saddle point.

Proof. Take Γ, the boundary of $\mathscr{D}_2$, as a Jordan curve (see Fig. 2). The index of Γ relative to the vector field $(f_1, f_2)^\top \in C^1(\mathbb{R}^2)$ is equal to 1, i.e. $I_{(f_1,f_2)^\top}(\Gamma) = 1$. Suppose system (3.2) has one interior saddle point E and other q interior equilibria $E_1, E_2, \ldots, E_q$. The index of E is -1 and that of $E_j (j = 1, 2, \ldots, q)$ equals $-1, 0$ or 1. According to the Index Theory (Perko, 2001, Theorem 2, p. 302), $I_{(f_1,f_2)^\top}(\Gamma) = I_{(f_1,f_2)^\top}(E) + \sum_{j=1}^{q} I_{(f_1,f_2)^\top}(E_j) = 1$, which means $\sum_{j=1}^{q} I_{(f_1,f_2)^\top}(E_j) = 2$. It then can be deduced that the minimum number of E_j is 2 whose index with respective to the vector field $(f_1, f_2)^\top$ equals 1. The proof is complete. □

THEOREM 3.10 Suppose $\beta > i$. If system (3.2) has a unique interior equilibrium (S_*, P_*), it is globally asymptotically stable.

Theorem 3.10 can be proved by using the same arguments as in the proof of Theorem 3.4 and adding the assumption of the uniqueness of the interior equilibrium to satisfy the conditions of Corollary 3.5 in Li (1996). Here, we omit the details.

The methods used to get the general results for $\beta > i$ are applicable to the case $\beta < i$. However, based on *in vitro* results (Portet *et al.*, 2009), it might be assumed here that $i \leqslant \beta$; the aggregation of short objects is faster than the aggregation of longer objects.

4. Discussion

A model for the organization of keratin material in a cell is proposed, describing the repartition of keratin between three structural states. Assumptions of the model result from biological observations (Kolsch *et al.*, 2010; Leube *et al.*, 2011). The model is based on keratin recycling (assembly/disassembly cycle); neither protein biosynthesis nor degradation are considered. Note that other modes of keratin filament turnover exist. They may rely on protein biosynthesis and protein degradation (Chang *et al.*, 2006; Rogel *et al.*, 2010) and include direct exchange between the soluble and filamentous keratin pools (Kreis *et al.*, 1983; Miller *et al.*, 1991).

As the *in vivo* mechanisms of the filament precursor formation (or the oligomerization of soluble proteins) are not very well understood, generic functions are used as nucleation functions. Saturating or non-saturating functions of the soluble pool are allowed as nucleation functions; the only assumption is a non-decreasing dependence on the available soluble proteins. The use of a generic function for the nucleation renders the mathematical analysis complicated. However, the present conclusions are in agreement with our previous conclusions (Portet & Arino, 2009) and biological observations (Kolsch *et al.*, 2010; Leube *et al.*, 2011).

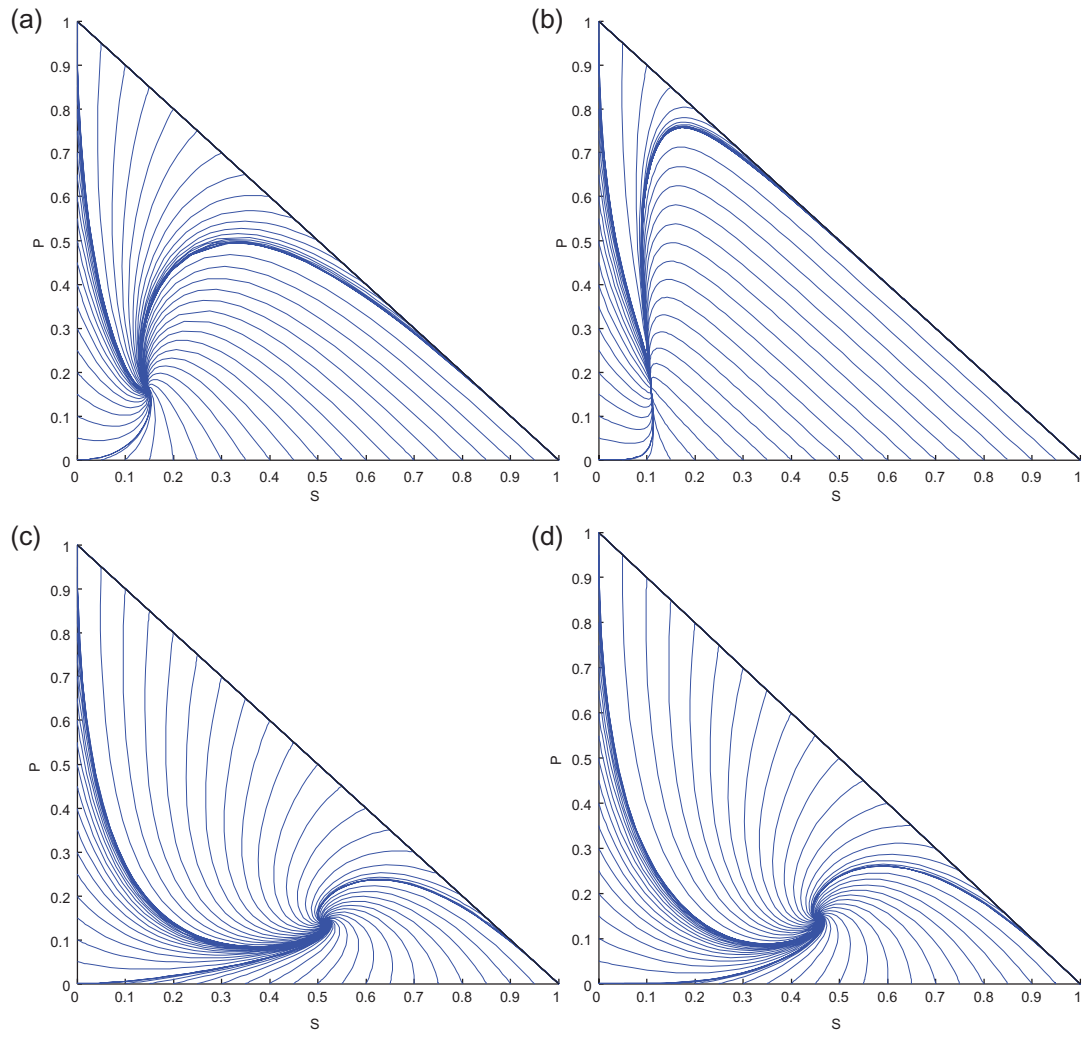

FIG. 3. Trajectories of system (3.2) considered with different nucleation functions converge to the unique interior equilibrium. The set of parameter values, such that $\beta = i$, is: $a = 0.5, b = 0.3 \times C_0, C_0 = 11, \pi = 2/(3 \times 60), \kappa = 20/(3 \times 60), \beta = i = 0.05, n = 3$. Four different nucleation functions are considered, all satisfying the properties defined in Section 2: (a) linear, $\mathcal{N}(C_0S) = aC_0S$; (b) exponential, $\mathcal{N}(C_0S) = aC_0^nS^n$; (c) Michaelis–Menten, $\mathcal{N}(C_0S) = aC_0S/(b + C_0S)$; (d) S-shaped, $\mathcal{N}(C_0S) = aC_0^nS^n/(b^n + C_0^nS^n)$. Depending on the nucleation function used, the values of the interior equilibrium change; saturating functions lead to a mainly soluble organization of the keratin material.

The rate κ of disassembly of the filamentous state is, as previously found in Portet & Arino (2009), one of the main determinants of the organization of the keratin material. The faster the disassembly, the smaller the proportion of material assembled in the filamentous state (Lemma 3.1). It is observed that once the network is assembled, its disassembly is triggered by post-transcriptional modifications of intermediate filament proteins due to the action of kinases (see, for example, Woll *et al.*, 2007). Hence, values of κ depend on the kinase activity that triggers filament disassembly.

The non-existence of periodic solutions is proved (Theorem 3.4). Additionally, since solutions are bounded and boundary equilibria are shown not to exist (Theorem 3.1), the keratin repartition always stabilizes, when time becomes large, to a steady state in which all structural stages always coexist. These conclusions are in agreement with biological observations; despite the continuous keratin assembly/disassembly, in interphasic cells, the repartition of keratin is stable in cells, 80% of the material is assembled in filamentous state (Windoffer *et al.*, 2011).

The formation of the filamentous state is described as a fusion/aggregation of filament precursors and aggregation of precursors to filaments (Kolsch *et al.*, 2010; Leube *et al.*, 2011). When fusion of precursors and integration of precursors into the filamentous pool are assumed to occur at the same rates ($\beta = i$), it is shown that the unique interior equilibrium (S_*, P_*) is globally asymptotically stable. Hence, the form of the nucleation function does not change the qualitative behaviour of the system. However, the use of saturating or non-saturating functions affects the (values of equilibrium solutions) repartition of the keratin material (see as an illustration Fig. 3). Of note, *in vitro* studies have shown that filament precursors, well identified as ULFs in the *in vitro* case, can be considered as filaments and that their rates of fusion are slightly higher than their rates of aggregation to filaments (Portet *et al.*, 2009). When $\beta \neq i$, it is difficult to determine analytically the number of interior equilibria (S_*, P_*) and the corresponding stability property.

Next steps of this study will include the transport of elements of keratin material in the different structural states and the localization of specific events in the cell.

Acknowledgements

The authors wish to thank the anonymous referee who provided the proof for the non-existence of periodic solutions without any condition (Theorem 3.4); this suggestion helped to improve the original manuscript.

Funding

This work was supported by the German Research Council (LE 566/18-1; WI 1731/8-1) and Natural Sciences and Engineering Research Council of Canada.

References

Bendixson, I. (1901) Sur les courbes définies par des équations différentielles. *Acta Math.*, **24**, 1–88.

Beriault, D. R., Haddad, O., McCuaig, J. V., Robinson, Z. J., Russell, D., Lane, E. B. & Fudge D. S. (2012) The mechanical behavior of mutant K14-R125P keratin bundles and networks in NEB-1 keratinocytes. *PLoS One*, **7**, e31320.

Carberry, K., Wiesenfahrt, T., Windoffer, R., Bossinger, O. & Leube. R. E. (2009) Intermediate filaments in Caenorhabditis elegans. *Cell Motil. Cytoskeleton*, **66**, 852–864.

Chang, L., Shav-Tal, Y., Trcek, T., Singer, R. H. & Goldman, R. D. (2006) Assembling an intermediate filament network by dynamic cotranslation. *J. Cell Biol.*, **172**, 747–758.

Colakoglu, G. & Brown, A. (2009) Intermediate filaments exchange subunits along their length and elongate by end-to-end annealing. *J. Cell Biol.*, **185**, 769–777.
Herrmann, H. & Aebi, U. (2004) Intermediate filaments: molecular structure, assembly mechanism, and integration into functionally distinct intracellular scaffolds. *Annu. Rev. Biochem.*, **73**, 749–789.
Herrmann, H., Bar, H., Kreplak, L., Strelkov, S. V. & Aebi, U. (2007) Intermediate filaments: from cell architecture to nanomechanics. *Nat. Rev. Mol. Cell Biol.*, **8**, 562–573.
Iwatsuki, H. & Suda, M. (2010) Transient expression of keratin during neuronal development in the adult rabbit spinal ganglion. *Anat. Sci. Int.*, **85**, 46–55.
Kim, S. & Coulombe, P. A. (2007) Intermediate filament scaffolds fulfill mechanical, organizational, and signaling functions in the cytoplasm. *Genes Dev.*, **21**, 1581–1597.
Kolsch, A., Windoffer, R., Wurflinger, T., Aach, T. & Leube, R. E. (2010) The keratin-filament cycle of assembly and disassembly. *J. Cell Sci.*, **123**, 2266–2272.
Kreis, T. E., Geiger, B., Schmid, E., Jorcano, J. L. & Franke, W. W. (1983) De novo synthesis and specific assembly of keratin filaments in nonepithelial cells after microinjection of mRNA for epidermal keratin. *Cell*, **32**, 1125–1137.
Leube, R. E., Moch, M., Kolsch, A. & Windoffer, R. (2011) "Panta rhei": Perpetual cycling of the keratin cytoskeleton. *Bioarchitecture*, **1**, 39–44.
Li, M. Y. (1996) Dulac criteria for autonomous systems having an invariant affine manifold. *J. Math. Anal. Appl.*, **199**, 374–390.
Magin, T. M., Vijayaraj, P. & Leube, R. E. (2007) Structural and regulatory functions of keratins. *Exp. Cell Res.*, **313**, 2021–2032.
Miller, R. K., Vikstrom, K. & Goldman, R. D. (1991) Keratin incorporation into intermediate filament networks is a rapid process. *J. Cell Biol.*, **113**, 843–855.
Oriolo, A. S., Wald, F. A., Ramsauer, V. P. & Salas, P. J. (2007) Intermediate filaments: a role in epithelial polarity. *Exp. Cell Res.*, **313**, 2255–2264.
Perko, L. (2001) *Differential Equations and Dynamical Systems*, 3rd edn. New York: Springer.
Portet, S. & Arino, J. (2009) An in vivo intermediate filament assembly model. *Math. Biosci. Eng.*, **6**, 117–134.
Portet, S., Mücke, N., Kirmse, R., Langowski, J., Beil, M. & Herrmann, H. (2009) Vimentin intermediate filament formation: in vitro measurement and mathematical modeling of the filament length distribution during assembly. *Langmuir*, **25**, 8817–8823.
Rogel, M. R., Jaitovich, A. & Ridge, K. M. (2010) The role of the ubiquitin proteasome pathway in keratin intermediate filament protein degradation. *Proc Am. Thorac. Soc.*, **7**, 71–76.
Sivaramakrishnan, S., Schneider, J. L., Sitikov, A., Goldman, R. D. & Ridge, K. M. (2009) Shear stress induced reorganization of the keratin intermediate filament network requires phosphorylation by protein kinase C zeta. *Mol. Biol. Cell*, **20**, 2755–2765.
Strnad, P., Windoffer, R. & Leube, R. E. (2001) In vivo detection of cytokeratin filament network breakdown in cells treated with the phosphatase inhibitor okadaic acid. *Cell Tissue Res.*, **306**, 277–293.
Strnad, P., Windoffer, R. & Leube, R. E. (2002) Induction of rapid and reversible cytokeratin filament network remodeling by inhibition of tyrosine phosphatases. *J. Cell Sci.*, **115**, 4133–4148.
Windoffer, R. Beil, M., Magin, T. M. & Leube, R. E. (2011) Cytoskeleton in motion: the dynamics of keratin intermediate filaments in epithelia. *J. Cell Biol.*, **194**, 669–678.
Windoffer, R., Woll, S., Strnad, P. & Leube, R. E. (2004) Identification of novel principles of keratin filament network turnover in living cells. *Mol. Biol. Cell*, **15**, 2436–2448.
Winheim, S., Hieb, A. R., Silbermann, M., Surmann, E.-M., Wedig, T., Herrmann, H., Langowski, J. & Mücke, N. (2011) Deconstructing the late phase of vimentin assembly by total internal reflection fluorescence microscopy (TIRFM). *PLoS One*, **6**, e19202.
Woll, S., Windoffer, R. & Leube, R. E. (2007) p38 MAPK-dependent shaping of the keratin cytoskeleton in cultured cells. *J. Cell Biol.*, **177**, 795–807.